Eur Biophys J (2009) 38:993–1002
DOI 10.1007/s00249-009-0491-4

ORIGINAL PAPER

Conformational rearrangements in the S6 domain and C-linker during gating in CNGA1 channels

Anil V. Nair · Chuong H. H. Nguyen · Monica Mazzolini

Received: 23 March 2009 / Revised: 7 May 2009 / Accepted: 13 May 2009 / Published online: 2 June 2009

Abstract This work completes previous findings and, using cysteine scanning mutagenesis (CSM) and biochemical methods, provides detailed analysis of conformational changes of the S6 domain and C-linker during gating of CNGA1 channels. Specific residues between Phe375 and Val424 were mutated to a cysteine in the CNGA1 and CNGA1$_{cys\text{-}free}$ background and the effect of intracellular Cd^{2+} or cross-linkers of different length in the open and closed state was studied. In the closed state, Cd^{2+} ions inhibited mutant channels A406C and Q409C and the longer cross-linker reagent M-4-M inhibited mutant channels A406C$_{cys\text{-}free}$ and Q409C$_{cys\text{-}free}$. Cd^{2+} ions inhibited mutant channels D413C and Y418C in the open state, both constructed in a CNGA1 and CNGA1$_{cys\text{-}free}$ background. Our results suggest that, in the closed state, residues from Phe375 to approximately Ala406 form a helical bundle with a three-dimensional (3D) structure similar to those of the KcsA; furthermore, in the open state, residues from Ser399 to Gln409 in homologous subunits move far apart, as expected from the gating in K^+ channels; in contrast, residues from Asp413 to Tyr418 in homologous subunits become closer in the open state.

Keywords Gating · CNGA1 channels · Cd^{2+} inhibition · Pore · S6 domain, C-linker

Abbreviations

CNG	Cyclic nucleotide-gated
CNBD	Cyclic nucleotide-binding domain
CSM	Cysteine scanning mutagenesis
MTS	Methanethiosulfonate
MTSET	2-(Trimethylammonium)ethyl] methanethiosulfonate bromide
MTSPT	3-(Trimethylammonium)propyl methanethiosulfonate bromide
MTS-PtrEA	3-(Triethylammonium)propyl methanthiosulfonate bromide
M-2-M	1,2-Ethanediyl bismethanethiosulfonate
M-4-M	1,4-Butanediyl bismethanethiosulfonate
M-6-M	1,6-Hexanediyl bismethanethiosulfonate

Introduction

Sensory transduction in vertebrate photoreceptors and olfactory sensory neurons is mediated by cyclic nucleotide-gated (CNG) channels (Fesenko et al. 1985; Zimmerman et al. 1985; Nakamura and Gold 1987; Kaupp et al. 1989; Biel et al. 1999; Zagotta and Siegelbaum 1996; Kaupp and Seifert 2002; Craven and Zagotta 2006). CNG channels form a tetrameric assembly of several homologous subunits (Chen et al. 1994; Körschen et al. 1995; Shammat and

Electronic supplementary material The online version of this article (doi:10.1007/s00249-009-0491-4) contains supplementary material, which is available to authorized users.

A. V. Nair · C. H. H. Nguyen · M. Mazzolini
International School for Advanced Studies,
via Beirut 2-4, 34014 Trieste, Italy

Present Address:
A. V. Nair
Department of Physiology, Nijmegen Centre for Molecular Life Sciences, Radboud University Nijmegen Medical Centre,
P.O. Box 9101, 6500 HB Nijmegen, The Netherlands

M. Mazzolini (✉)
International School for Advanced Studies, Area Science Park
SS 14 Km 163.5 Edificio Q1 Basovizza (TS),
34012 Trieste, Italy
e-mail: mazzolin@sissa.it

Gordon 1999; Zhong et al. 2002; Zheng et al. 2002; Craven and Zagotta 2006), usually referred to as CNGA1–CNGA4, CNGB1, and CNGB3 (Bradley et al. 2001). The amino acid sequence of CNG and K^+ channels share a significant homology (Zagotta and Siegelbaum 1996; Biel et al. 1999) and it has been hypothesized that CNG and K^+ channels have the same 3D topology and gating mechanism. The 3D structure of several K^+ channels has already been solved in the past: KcsA in the closed state (Doyle et al. 1998), MthK in the open state (Jiang et al. 2002a, b), KirBac 1.1 (Kuo et al. 2003), and mammalian Kv1.2 (Long et al. 2005). In all these K^+ channels the pore domain includes four identical subunits comprising two transmembrane helices, S5 and S6 (TM1 and TM2 in KcsA and MthK channels), a loop forming the filter region, and an additional small helix, not spanning the lipid membrane referred to as the P-helix. In K^+ channels, the major structural difference on passing from the closed to the open conformation is the bending of the S6 helix towards the lipid phase by 30° around a glycine hinge corresponding to Gly83 in MthK and Gly99 in KcsA (Jiang et al. 2002a, b).

The analysis of residue accessibility in the pore of CNG channels, based on the cysteine CSM method (Akabas et al. 1992; Kurz et al. 1995; Benitah et al. 1996; Krovetz et al. 1997; Karlin and Akabas 1998), has shown that CNG and K^+ channels share the same gross topology (Becchetti et al. 1999). A similar analysis performed in the S6 domain of CNGA1 channels from Val384 to Ser399 (Flynn and Zagotta 2001, 2003) suggested that also in CNG channels this domain has a helical configuration, possibly crossing at a hypothetical constriction located between residue Val391 and Ser399. On the basis of their results Flynn and Zagotta (2003) proposed that the closed and open conformations of the CNGA1 channels are similar to the 3D structure of KcsA and MthK, respectively. Another work based on CSM method, using the oxidizing agent CuP (Hua and Gordon 2005), concluded that residues from Gln417 to Val424 in neighboring subunits become closer in the open state and are far apart in the closed state. Therefore, during channel gating, residues in homologous subunits from Val384 and Ser399 move away from each other in a different way from the residues from Gln417 to Val424.

The purpose of the present study is to verify and extend previous investigations (Flynn and Zagotta 2001, 2003; Hua and Gordon 2005; Giorgetti et al. 2005; Mazzolini et al. 2008; Nair et al. 2009) on the spatial rearrangement of amino acids during gating in the S6 domain and in the initial portion of the C-linker, focusing in particular on understanding the relative motion of residues from Ser399 to Gln417. Specific residues between Phe375 and Val424 were mutated to a cysteine in the CNGA1 and CNGA1$_{cys\text{-}free}$ background; modifications induced by intracellular Cd^{2+} (Mazzolini et al. 2002; Rothberg et al. 2002, 2003) were analyzed in these mutant channels in the open and closed state, and the effect of other sulfhydryl reagents, such as 2-(trimethylammonium)ethyl methanethiosulfonate bromide (MTSET) and methanethiosulfonate (MTS) cross-linkers (Loo and Clarke 2001), was investigated on selected mutants.

Materials and methods

Molecular biology and electrophysiology

Two different channel constructs from bovine rods were used: the CNGA1 channel, consisting of 690 residues (about 80 kDa), and the CNGA1$_{cys\text{-}free}$ channel, without any endogenous cysteines (Matulef et al. 1999). Selected residues were mutated in cysteine. Oocytes preparation, recording apparatus, and application of sulfhydryl-specific reagents were the same as previously described (Mazzolini et al. 2008; Nair et al. 2009). The methanethiosulfonate (MTS) compounds were purchased from Toronto Research Chemicals (Ontario, Canada) whereas the other chemicals were from Sigma Chemicals (St. Louis, MO, USA).

Estimation of the distance between C_α of coordinating cysteines

The method for the determination of Cd^{2+} action on exogenous cysteines and the time course of inhibition is explained in detail in the Supplementary Material section and in Fig. S1.

The distance between the C_α of cysteines coordinating Cd^{2+} ions or cross-linkers such as 1,2-ethanediyl bismethanethiosulfonate (M-2-M) and 1,4-butanediyl bismethanethiosulfonate (M-4-M) was estimated, as previously described (Mazzolini et al. 2008). We calculated that, if Cd^{2+} inhibits the channel by coordinating to two cysteines, the distance between the C_α of coordinating cysteines is $\leq$10.5 Å. If channel inhibition is observed with M-2-M but not with Cd^{2+} the distance between the C_α of coordinating cysteines is between 10.5 and 12.3 Å. Similarly, if the inhibition is caused by M-4-M and not by Cd^{2+} and M-2-M, the distance between the C_α of coordinating cysteines is between 12.3 and 14.7 Å (Mazzolini et al. 2008; Nair et al. 2009).

Protein preparation and immunoblotting

The effect of MTS-X-MTS compounds in the closed and open state was investigated also with biochemical methods using protein isolation and immunoblotting in order to ascertain whether the effect observed in the electrophysiological experiments was confirmed by the formation of

dimers after the addition of these cross-linkers. After channel expression, oocytes were prepared based on the method described by Nair et al. (2009). In the closed state, the oocytes expressing the $CNGA1_{cys\text{-}free}$, $A406C_{cys\text{-}free}$, and $Q409C_{cys\text{-}free}$ RNA were homogenized (with and without MTS reagents, without cGMP); MTS reagents were added to the homogenization buffer (final concentration 5 mM) immediately before homogenizing the oocytes. In the open state (based on the method of Rosenbaum and Gordon 2002), 24 h before the homogenization, oocytes were injected with 2 mM cGMP and 5 mM MTS-X-MTS compounds, or only with cGMP, then the oocytes were incubated at 19°C in solution containing cGMP and MTS-X-MTS. The samples were loaded in absence or presence of 10% v/v β-mercaptoethanol (β-ME) or 100 mM dithiothreitol (DTT) and subjected to sodium dodecyl sulfate polyacrylamide gel electrophoresis (SDS-PAGE) using 3–8% acrylamide gel; channels were detected with Western blotting using a mouse M2 anti-FLAG primary antibody (Sigma-Aldrich) and an anti-mouse IgG secondary antibody conjugated with horseradish peroxidase (HRP) (GE Healthcare).

Results

The modifications caused by intracellular Cd^{2+} and other sulfhydryl reagents, such as MTSET and MTS cross-linkers (Loo and Clarke 2001), were investigated in presence (open state) and absence (closed state) of 1 mM cGMP when residues in the S6 domain and C-linker were mutated to cysteines in CNGA1 and in $CNGA1_{cys\text{-}free}$ background.

These regions can be divided into three segments with different properties (Fig. 1): (1) the first segment, from Phe375 to Ser399, where the effect of Cd^{2+} ions in mutant channels constructed in the CNGA1 is very similar in the closed and open state; (2) the second segment, from Asn400 to Glu409, in which Cd^{2+} ions inhibited in the closed state many mutant channels constructed in the CNGA1 background but not in $CNGA1_{cys\text{-}free}$ background; and (3) the third segment, from Ala410 to Val424, where the effect of Cd^{2+} ions was similar for some, but not all, of the mutant channels constructed in the CNGA1 and $CNGA1_{cys\text{-}free}$ background.

Cd^{2+} effect on mutant channels from F375C to S399C

At +60 mV, 100 μM Cd^{2+} ions did not inhibit mutant channels from F375C to S399C in either the open or closed state, with the exception of mutant channels F380C and V391C (Giorgetti et al. 2005). Indeed, partial inhibition in the closed state (0.38 ± 0.16, $n = 7$) was observed in mutant channel F380C (see also Nair et al. 2006), which was potentiated in the open state (-0.37 ± 0.15, $n = 7$); in mutant channel V391C clear inhibition was observed in both the closed (0.83 ± 0.11, $n = 5$) and open state (0.83 ± 0.1, $n = 5$). At −100 mV, when 10 or 100 μM Cd^{2+} was added to the medium in presence or absence of 1 mM cGMP, the cGMP-activated current in mutant channel V391C was quickly suppressed (Fig. 2a, b), in contrast with what was observed for the WT (wild type) CNGA1 channel (Becchetti and Roncaglia 2000). This powerful inhibition at very negative voltage indicates binding to exogenous cysteines. Cd^{2+} (100 μM) inhibited the mutant channel V391C in less than 5 s, whereas concentration lower than 100 nM in the open state and 1 μM in the closed state did not produce any inhibition (Fig. 2a, b). Using a single exponential fit (in red), we calculated the time constant τ of current recovery after application of 100 μM Cd^{2+} in the open and closed state. Our results indicate a value of τ equal to 6.5 ± 0.02 and 19.1 ± 0.12 s in the open and closed state, respectively (Fig. 2c, d).

The stoichiometry of Cd^{2+} inhibition (Fig. 2a, b) was fitted by the equation (Rothberg et al. 2003)

$$1 - I_{res}/I_{cGMP} = 1/\{1 + (K_{1/2}/[Cd^{2+}])\}^n, \quad (1)$$

where I_{res} is the residual current measured in presence of 1 mM cGMP after Cd^{2+} application, I_{cGMP} is the cGMP-activated current in the absence of Cd^{2+}, n is the Hill coefficient, $K_{1/2}$ is the Cd^{2+} concentration inhibiting 50% of I_{cGMP}, and $[Cd^{2+}]$ is the cadmium concentration. Our results indicate that, in the open state, the value of $K_{1/2}$ is 330 ± 5 nM with n equal to 3, but in the closed state $K_{1/2}$ is equal to 2.5 ± 0.03 μM with $n = 3$. Our results are very similar to those observed by Rothberg et al. (2003) in the double mutant H462Y + Q468C of the spHCN channel, where Cd^{2+} inhibition in the closed state is described by the same equation (1) with a value of the Hill coefficient equal to 4. A value of n larger than 1 indicates

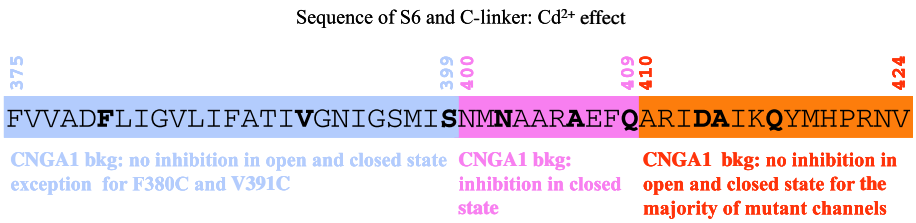

Fig. 1 Sequence of the S6 and C-linker regions. Schematic representation of Cd^{2+} effect and relative subdivision into three segments: from 375 to 399 in violet, from 400 to 409 in pink, and from 410 to 424 in orange. *Bkg* background

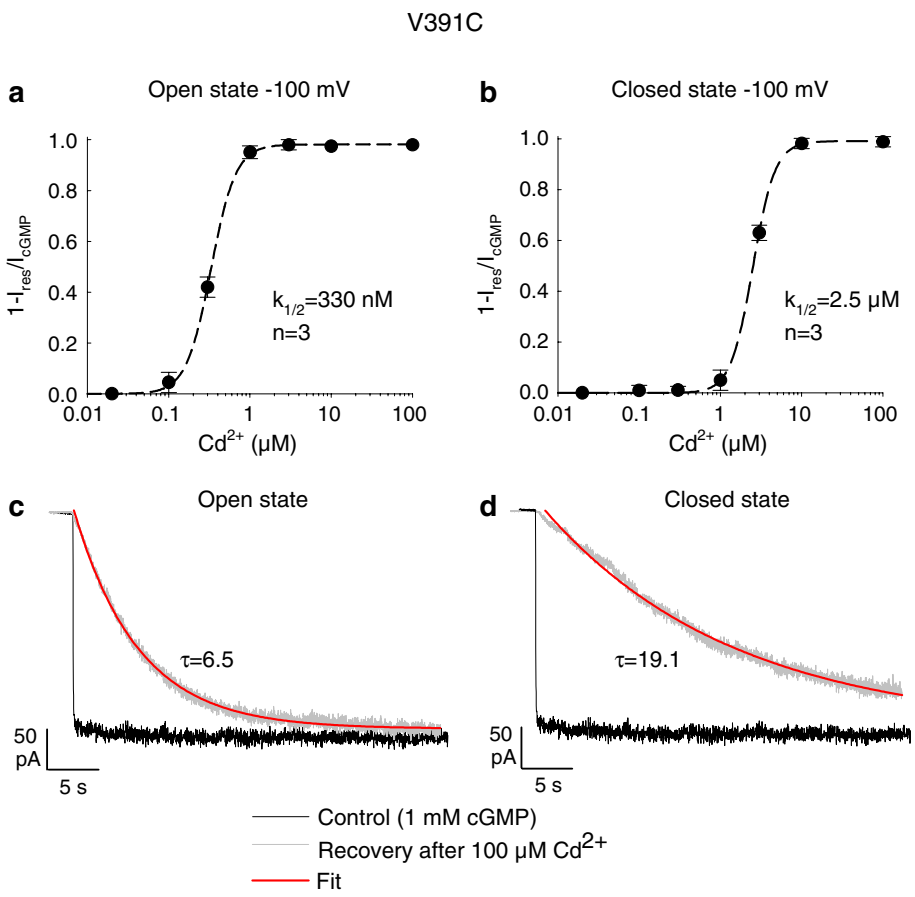

Fig. 2 Effect of Cd^{2+} on mutant channel V391C. **a** Stoichiometry of Cd^{2+} inhibition in presence of 1 mM cGMP at −100 mV; line through the experimental points was obtained using a sigmoidal equation with values of $n = 3$ and $K_{1/2} = 330 \pm 5$ nM; values are shown as mean ± standard deviation (SD). **b** As in (**a**) but in absence of cGMP; line through the experimental points was obtained using a sigmoidal equation with values of $n = 3$ and $K_{1/2} = 2.5 \pm 0.03$ μM. (**c**–**d**) Comparison between control current in presence of 1 mM cGMP (*black*) and current recovery after exposure of 100 μM Cd^{2+} (*gray*) in open and closed state at −100 mV; in *red*, single exponential fit of current recovery time constant in the open state ($\tau = 6.5 \pm 0.02$ s) and in the closed state ($\tau = 19.1 \pm 0.12$ s)

cooperativity among Cd^{2+} ions, suggesting that several Cd^{2+} ions coordinate to exogenous cysteines at location 391.

The cGMP-activated current for mutant channel S399C declined spontaneously in the closed (as already reported, Flynn and Zagotta 2001) but also in the open state. The rundown in the open state was variable: in 12 out of 28 patches the run down was less than 10%, but in the remaining patches the cGMP-activated current declined within 7–15 min to a steady level between 20% and 25% of the initial current. Since the effect of Cd^{2+} on mutant channels from F375C to S399C in the closed and open state is very similar, no mutant channels were constructed in the $CNGA1_{cys\text{-}free}$ background.

Cd^{2+} inhibition in mutant channels from N400C to Q409C

As reported in Giorgetti et al. (2005) many mutant channels from N400C to Q409C were powerfully and irreversibly inhibited in the closed state: at +60 mV, 100 μM Cd^{2+} ions powerfully inhibited mutant channels N402C (0.8 ± 0.12, $n = 4$), A403C (0.82 ± 0.16, $n = 5$), A406C (0.85 ± 0.13, $n = 8$), and Q409C (0.98 ± 0.02, $n = 7$). In contrast, in the open state, 100 μM Cd^{2+} did not inhibit these mutant channels.

In order to explore the molecular mechanism responsible for Cd^{2+} inhibition of mutant channels described before, we introduced cysteine at specific locations also in the $CNGA1_{cys\text{-}free}$ background (Matulef et al. 1999). We analyzed the effect of 100 μM Cd^{2+} ions in mutant channels $N400C_{cys\text{-}free}$ ($n = 3$), $N402C_{cys\text{-}free}$ ($n = 3$), $A406C_{cys\text{-}free}$ ($n = 4$), $E407C_{cys\text{-}free}$ ($n = 3$), and $Q409C_{cys\text{-}free}$ ($n = 4$). As summarized in Fig. 3a, none of these mutant channels was inhibited by 100 μM Cd^{2+}, neither in the open nor in the closed state.

Cd^{2+} inhibition in mutant channels from A410C to V424C

As reported in a previous work (Giorgetti et al. 2005) mutant channels from A410C to V424C, with the exception of R411C, N423C, and V424C, were all functional and a cGMP-activated current with amplitude and properties similar to those observed in the CNGA1 was measured. However, an unexpected behavior was observed for mutant channel D413C. As illustrated in Fig. 3b, in this mutant channel at ±60 mV in presence of 1 mM cGMP, we

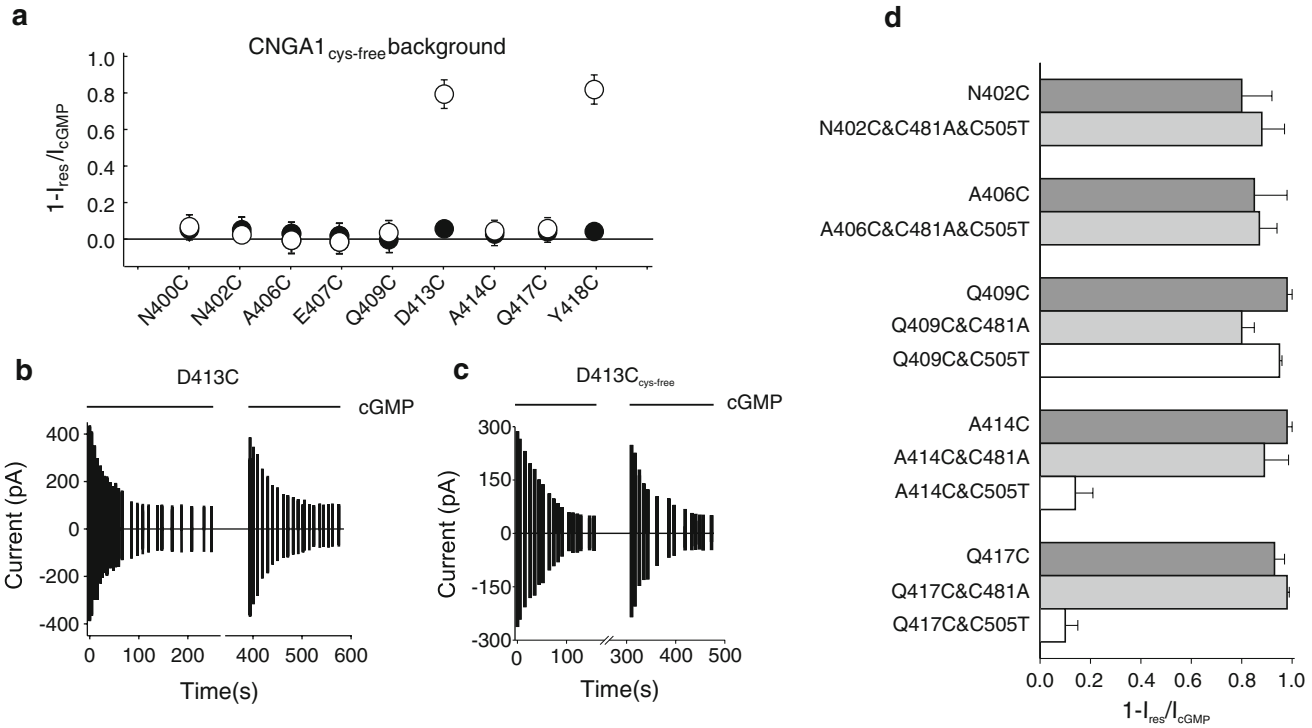

Fig. 3 Cd^{2+} modification from residues N400C to Y418C. **a** Fractional change induced by 100 μM Cd^{2+} at +60 mV for mutant channels constructed in the $CNGA1_{cys\text{-}free}$ background. Effect of 100 μM Cd^{2+} added for 5 min in absence (*black circles*) and presence of 1 mM cGMP (*white circles*). **b–c** Reversible current decline of mutant channels D413C and $D413C_{cys\text{-}free}$; *vertical bars* indicate the current at ±60 mV in presence of 1 mM cGMP. By removing cGMP for at least 3 min a cGMP-activated current with the same amplitude as originally observed could be measured for both mutant channels D413C and $D413C_{cys\text{-}free}$. **d** Role of endogenous cysteines in position 481 and 505 for mutant channels constructed in the CNGA1 background: the Cd^{2+} inhibition in mutant channels N402C, A406C, Q409C, A414C, and Q417C is compared when Cys481 and Cys505 were replaced with an alanine and a threonine, respectively. All values obtained at +60 mV in the closed state. Values are shown as mean ± SD

observed a progressive decline of current, reaching a value that was approximately 40% of that initially observed. When cGMP was removed from the medium for at least 90 s, a subsequent exposure to 1 mM cGMP activated a current with the same original amplitude. This behavior is very similar but not identical to the desensitization observed in mutant channels E363A, T355A, L356A, and F380A (Bucossi et al. 1996; Roncaglia and Becchetti 2001; Giorgetti et al. 2005, Mazzolini et al. 2009). Desensitization of the cGMP-activated current was also observed in mutant channel $D413C_{cys\text{-}free}$ (Fig. 3c), where the current declined, in a reversible way, to about 20% of the value measured immediately after the addition of cGMP.

For these reasons, the action of Cd^{2+} ions on mutant channels D413C and $D413C_{cys\text{-}free}$ was tested when the cGMP-activated current was fully desensitized. As shown in Fig. 3d and as previously reported (Giorgetti et al. 2005) Cd^{2+} ions powerfully inhibited mutant channels A414C (0.98 ± 0.02, $n = 5$) and Q417C (0.93 ± 0.04, $n = 4$) in the closed state, but not in the open state. In the open state, Cd^{2+} ions inhibited mutant channels D413C (0.81 ± 0.1, $n = 3$) and Y418C (0.89 ± 0.1 $n = 3$). The mutant channel H420C was not affected by Cd^{2+} ions in presence of 1 mM cGMP (0.05 ± 0.05, $n = 3$) and was poorly inhibited when exposed to Cd^{2+} in absence of cGMP (0.17 ± 0.03, $n = 4$). Cd^{2+} inhibition observed in the closed state in mutant channels A414C and Q417C was not observed when cysteines were introduced in the $CNGA1_{cys\text{-}free}$ background (Fig. 3a). Cd^{2+} inhibition in the open state was observed in mutant channels $D413C_{cys\text{-}free}$ (0.78 ± 0.05, $n = 4$) and $Y418C_{cys\text{-}free}$ (0.81 ± 0.05, $n = 5$) (Fig. 3a).

Role of Cys481 and Cys505 in Cd^{2+} inhibition

The different blocking effects of Cd^{2+} ions can be produced by two different mechanisms or by their combination. According to mechanism 1, Cd^{2+} inhibition of the cysteine mutant channel in the CNGA1 background can originate from Cd^{2+} coordination to the exogenous cysteine with endogenous cysteines and particularly with Cys481 and/or Cys505, which are part of the C-linker domain (Brown et al. 1998). An alternative explanation (mechanism 2) is that the 3D structure of $CNGA1_{cys\text{-}free}$

channels differs by some Å from that of CNGA1 channels, so that Cd^{2+} can coordinate exogenous cysteines introduced in the CNGA1 background but not in the $CNGA1_{cys\text{-}free}$ background. If in these experiments Cd^{2+} inhibition was drastically reduced or eliminated, mechanism 1 could be validated. In the second series of experiments the effect of cross-linkers of different length in mutant channels $A406C_{cys\text{-}free}$ and $Q409C_{cys\text{-}free}$ was examined. The existence of MTS cross-linkers (Loo and Clarke 2001) able to block mutant channels irreversibly in the closed state could support mechanism 2.

As shown in Fig. 3d (see also Mazzolini et al. 2008; Nair et al. 2009), Cd^{2+} inhibition (100 μM), in the closed state at +60 mV, was observed in mutant channels N402C (0.95 ± 0.04, $n = 4$) and A406C (0.98 ± 0.02, $n = 7$) as well as in the triple mutant channels N402C&C481A &C505T (0.88 ± 0.09, $n = 4$) and A406C&C481A& C505T (0.87 ± 0.07, $n = 5$). Similarly, as shown in Fig. 3d, in mutant channels Q409C&C505T and Q409C& C481A, exposure to Cd^{2+} resulted in inhibition of 0.95 ± 0.01 ($n = 5$) and 0.8 ± 0.05 ($n = 6$), respectively. The rate of Cd^{2+} inhibition was very similar in all these mutant channels, indicating that presence of native cysteines Cys481 and Cys505 does not contribute to Cd^{2+} inhibition in mutant channels N402C, A406C, and Q409C, in contrast with what was observed for mutant channels A414C and Q417C. Indeed, as shown in Fig. 3d, Cd^{2+} inhibition in mutant channels A414C (0.98 ± 0.02, $n = 4$) and Q417C (0.96 ± 0.01, $n = 5$) was eliminated in the double mutants A414C&C505T (0.14 ± 0.07, $n = 6$) and Q417C&C505T (0.1 ± 0.05, $n = 4$) but not in the double mutants A414C&C481A (0.89 ± 0.09, $n = 6$) and Q417C&C481A (0.98 ± 0.009, $n = 4$). In mutant channels A414C and Q417C, Cd^{2+} inhibition was insensitive to presence of Cys481, but was almost abolished when native Cys505 was replaced with a threonine.

These results suggest that Cd^{2+} inhibition in the closed state observed for mutant channels N402C, A406C, and Q409C is primarily mediated by Cd^{2+} binding to exogenous cysteines, whereas in mutant channels A414C and Q417C, Cd^{2+} inhibition is also mediated by Cd^{2+} binding to native Cys505.

The effect of MTS cross-linkers on mutant channels $A406C_{cys\text{-}free}$ and $Q409C_{cys\text{-}free}$

As described, Cd^{2+} ions in absence of cGMP powerfully inhibited mutant channels A406C and Q409C but not mutant channel $A406C_{cys\text{-}free}$ and $Q409C_{cys\text{-}free}$ (Fig. 3a, see also Mazzolini et al. 2008; Nair et al. 2009). To determine which molecular mechanisms cause this different effect by Cd^{2+} ions we investigated inhibition by different thiol cross-linkers of MTS-X-MTS family with an increasing length of the linker. Cross-linker M-2-M (100 μM) did not block mutant channels $A406C_{cys\text{-}free}$ and $Q409C_{cys\text{-}free}$ in either the open (0.02 ± 0.05 $n = 6$; 0.03 ± 0.05 $n = 6$) or the closed state (0.07 ± 0.07, $n = 5$; 0.37 ± 0.2, $n = 4$). In contrast, the same concentration of the reagent M-4-M powerfully inhibited both mutant channels $A406C_{cys\text{-}free}$ (0.94 ± 0.02, $n = 7$) and $Q409C_{cys\text{-}free}$ (0.83 ± 0.014, $n = 5$) in the closed state but not in the open state (0.19 ± 0.13, $n = 4$; 0.04 ± 0.038, $n = 3$), as shown in Fig. 4a and b, respectively. The reagent M-6-M inhibited rather powerfully the mutant channel $A406C_{cys\text{-}free}$ (0.85 ± 0.05, $n = 3$) but not the mutant channel $Q409C_{cys\text{-}free}$ (0.07 ± 0.07, $n = 3$) in the open state.

The observed inhibition of mutant channels $A406C_{cys\text{-}free}$ and $Q409C_{cys\text{-}free}$ by cross-linkers prompted us to think that it could be caused by a simple steric occlusion and not by the cross-linking of the two exogenous cysteines. We then compared the blocking effect of different MTS compounds such as 100 μM MTSEA, MTSET, MTSPT, and MTSPtrEA on the mutant channels $A406C_{cys\text{-}free}$ and $Q409C_{cys\text{-}free}$ (Fig. 4c–d): none of these large MTS compounds significantly blocked both mutant channels $A406C_{cys\text{-}free}$ ($n = 5$) and $Q409C_{cys\text{-}free}$ ($n = 5$). These data confirm that the observed inhibition is caused by the coordination of cross-linkers to two cysteines.

To confirm the state-dependent blockage by M-4-M and M-6-M of mutant channels $A406C_{cys\text{-}free}$ and $Q409C_{cys\text{-}free}$ observed in electrophysiological recordings (Mazzolini et al. 2008; Nair et al. 2009), we analyzed the effect of cross-linkers (Fig. 4e–f) with biochemical methods, based on the use of protein extraction and immunoblotting. Therefore we extracted the protein constituting mutant channels in different conditions and by using appropriate antibodies we determined their molecular weight. In this way we could determine whether the protein forms monomers and/or also dimers. The formation of dimers indicates that the cross-linkers bound two subunits of the channel (Loo and Clarke 2001; Craven et al. 2008), representing the biochemical equivalent of the inhibition of the cGMP-gated current observed in electrophysiological experiments.

As expected from the electrophysiological results, in the closed but not in the open state and in the presence of M-4-M the protein runs on the gel with the size of a dimer (about 160 kDa) for both mutant channels $A406C_{cys\text{-}free}$ (Fig. 4e) and $Q409C_{cys\text{-}free}$ (Fig. 4f). In the presence of the longer cross-linker M-6-M, the formation of dimers of mutant channel $Q409C_{cys\text{-}free}$ (Fig. 4f) was observed only in the closed state but not in the open state. In contrast, the formation of dimers of mutant channel $A406C_{cys\text{-}free}$ was observed in both the open and closed states (Fig. 4f). The dimer formation is reverted in reducing conditions (10% v/v

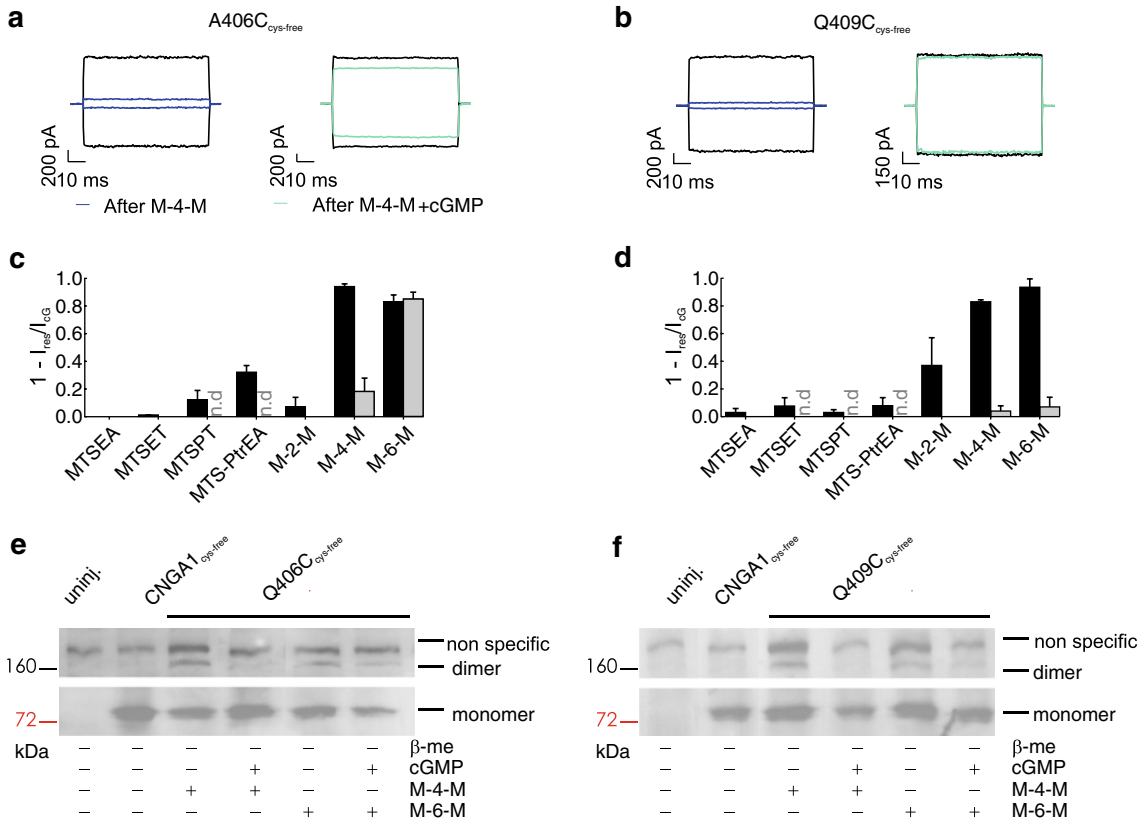

Fig. 4 Effect of cross-linkers in $A406C_{cys\text{-}free}$ and $Q409C_{cys\text{-}free}$ mutants. M-4-M effect in $A406C_{cys\text{-}free}$ (**a**) and $Q409C_{cys\text{-}free}$ (**b**) in the open (*right panels*) and closed (*left panels*) states at ±60 mV. *Blue traces* are the effect after the cross-linker application and *cyan traces* are after the open-state application. *Black traces* are before the application of the cross-linker. Effect of different cross-linking and other MTS reagents on mutant channels $A406C_{cys\text{-}free}$ (**c**) and $Q409C_{cys\text{-}free}$ (**d**) at +60 mV. *Black bars* show the effect of MTS reagents applied in the closed state; *grey bars* show after the open state. Values are shown as mean ± SD. Biochemical analysis of mutant channels $A406C_{cys\text{-}free}$ (**e**) and $Q409C_{cys\text{-}free}$ (**f**): Western blots of total proteins from *Xenopus* oocytes in nonreducing conditions performed in oocytes uninjected or injected with mRNA of $CNGA1_{cys\text{-}free}$ channels (control), and $A406C_{cys\text{-}free}$ (**e**) and $Q409C_{cys\text{-}free}$ (**f**) mutant channels

β-me or 100 mM DTT), where only monomers are observed (data not shown). In each considered condition we observed a nonspecific protein (present also in uninjected oocytes) that runs on the gel with size >160 kDa, as indicated in Fig. 4e–f. Electrophysiological and biochemical data shown in Fig. 4 show that the compound M-4-M inhibited mutant channels $A406C_{cys\text{-}free}$ and $Q409C_{cys\text{-}free}$ in the closed but not in the open state.

Discussion

The present results verify and complete our previous findings (Giorgetti et al. 2005; Mazzolini et al. 2008; Nair et al. 2009), provide new experimental information on the 3D structure of the S6 domain and C-linker, and contribute to understanding of the molecular mechanisms underlying gating in CNGA1 channels (Johnson and Zagotta 2001; Flynn and Zagotta 2001; Flynn and Zagotta 2003; Giorgetti et al. 2005; Hua and Gordon 2005). We confirm that residues from Phe375 to Ser399 have an alpha-helix conformation (Flynn and Zagotta 2001, 2003) with a spatial arrangement referred to as "an inverted tee-pee" (Doyle et al. 1998), as expected from the homology with all other ionic channels for which the 3D structure has been solved (Jiang et al. 2002a, b; Kuo et al. 2003; Long et al. 2005). As mutant channels A406C and Q409C are irreversibly inhibited by Cd^{2+} in the closed but not in the open state, and mutant channels $A406C_{cys\text{-}free}$ and $Q409C_{cys\text{-}free}$ are inhibited by M-4-M with the same state dependency, residues from positions 406 and 409 in different subunits are near each other in the closed state but move apart in the open state. These findings suggest that, in the closed state, residues from Phe375 to approximately Ala406 form a helical bundle with a 3D structure similar to those of the KcsA and that, in the open state, residues from Ser399 to Gln409 in homologous subunits move far apart, as expected from the gating in K^+ channels. A different behavior

was instead observed for mutant channels D413C and Y418C and for mutant channels $D413C_{cys\text{-}free}$ and $Y418C_{cys\text{-}free}$, which are inhibited by Cd^{2+} ions in the open but not in the closed state, in agreement with a previous report (Hua and Gordon 2005). These experimental results are not in agreement with our previous proposed model (Giorgetti et al. 2005) and suggest a modification of it, presented in Fig. 5.

Residues from Phe375 to Ser399

Cd^{2+} inhibition of mutant channels from F375C to S399C is very similar in both the open and closed state (Giorgetti et al. 2005), with the exception of mutant channels F380C and V391C (Fig. 2, see also Giorgetti et al. 2005; Nair et al. 2006). Mutant channel F380C exhibited a partial inhibition in the closed state and a potentiation in the open state caused by interactions with Cys314 in the S5 helix (Nair et al. 2006). The effect of sulfhydryl reagents in this mutant channel was very similar when constructed in the CNGA1 and $CNGA1_{cys\text{-}free}$ background (Nair et al. 2006). Mutant channel V391C constructed in the CNGA1 was powerfully blocked by Cd^{2+} ions in both the open and closed state, with $K_{1/2} = 330$ nM and 2.5 μM, respectively (Fig. 2a–b). These results suggest that Val391 in different subunits are close to each other in both the open and closed state, and that mutant channel V391C has an easily accessible binding site for Cd^{2+} ions in which three or four Cd^{2+} ions coordinate to four S atoms with a molecular mechanism similar to that proposed by Rothberg et al. (2003) for the double mutant H462Y + Q498C in spHCN channels, in which Cd^{2+} inhibition is very potent with a value of $K_{1/2}$ of 72 nM (Rothberg et al. 2003). We have observed a spontaneous rundown of the cGMP-activated current in mutant channel S399C in the open and closed state, suggesting that Ser399 in homologous subunits are near to each other and disulphide bonds can form spontaneously in mutant channels S399C in both the open and closed state. All these observations indicate that the 3D structure of the MthK channel is not a good template for the spatial arrangement of residues from Val384 to Ser399 in the open state as originally proposed (Flynn and Zagotta 2001; Flynn and Zagotta 2003).

Residues from Asn400 to Gln409

Mutant channels N400C, N402C, A403C, A404C, A406C, E407C, and Q409C are powerfully blocked in the closed state in the CNGA1 background (see Giorgetti et al. 2005), but not in the $CNGA1_{cys\text{-}free}$ (Fig. 3a). None of these mutant channels are blocked in the open state, in either the CNGA1 or the $CNGA1_{cys\text{-}free}$ background. Mutant channels A406C and Q409C are irreversibly inhibited by Cd^{2+} in the closed but not in the open state. When cysteines were introduced in positions 406 and 409 in the $CNGA1_{cys\text{-}free}$ background no Cd^{2+} inhibition was observed, but M-4-M (Fig. 4a–b) irreversibly inhibited both mutant channels $A406C_{cys\text{-}free}$ and $Q409C_{cys\text{-}free}$ in the closed but not in the open state. Therefore, homologous residues at both positions 406 and 409 are near each other in the closed state but

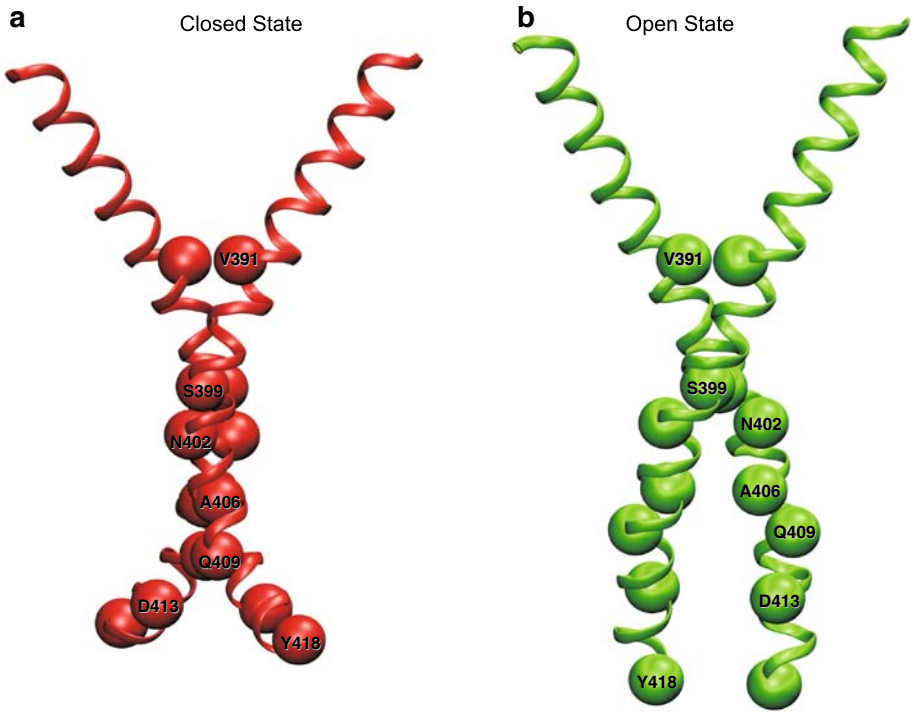

Fig. 5 Model of possible movement of the S6-C-linker transmembrane helices of CNG channel. In *red*, front view of closed state (**a**) and in *green*, front view of open state (**b**). The residues from Asn400 to Gln409 are near in the closed state (*red*) and residues from Asp413 to Tyr418 are near in the open state (*green*). For clarity only two subunits are shown

during channel opening they undergo a significant conformation rearrangement in which residues at position 409 are further apart than those at position 406. These results are also confirmed from Western blot analysis (Fig. 4e–f).

Residues from Ala410 to Val424

Mutant channels A414C and Q417C were blocked by Cd^{2+} ions in the closed state in the CNGA1 background (Fig. 3d) but not in the $CNGA1_{cys\text{-}free}$ (Fig. 3a). However Cd^{2+} inhibition was significantly reduced when native Cys505 was replaced with a threonine. This indicates that Cd^{2+} inhibition in mutant channels A414C and Q417C is not primarily caused by its coordination to exogenous cysteines in distinct subunits, but by its coordination to exogenous cysteines and to the native Cys505, possibly in the same subunit. Mutant channels D413C and Y418C were inhibited by Cd^{2+} ions in the open state but not in the closed state (Giorgetti et al. 2005). A similar result was observed for mutant channels $D413C_{cys\text{-}free}$ and $Y418C_{cys\text{-}free}$ (Fig. 3a). Thus, in agreement with Johnson and Zagotta (2001) and Hua and Gordon (2005), we conclude that homologous residues in different subunits from Asp413 to Tyr418 move closer in the open state.

The structure of the S6 domain and initial portion of the C-linker in the closed and open states

These experimental observations can be rationalized in the molecular model presented in Fig. 5. This model assumes that, in the closed state, residues from Phe375 to His420 have an alpha-helix conformation. Mutant channels V391C are inhibited by Cd^{2+} ions in both the closed and open state, and a spontaneous rundown of the cGMP-activated current of mutant channels S399C is observed in both the closed and open state. These results suggest that residues from Phe375 to Ser399 in homologous subunits are near each other in the closed state and remain at a close distance also during channel gating.

Residues in homologous subunits from Ala400 to Gln409 are near each other in the closed state (Fig. 5a) but at a relative greater distance than Val391 because of a reduced efficiency of Cd^{2+} inhibition. Mutant channels A406C and Q409C are not blocked by Cd^{2+} ions in the open state, suggesting that residues from Ala400 to Gln409 move apart in the open state (Fig. 5b). In contrast, mutant channels D413C and Y418C were inhibited by Cd^{2+} ions in the open state but not in the closed state, suggesting that residues from Asp413 to Tyr418, move differently: these residues are nearer each other in the open state (Fig. 5b).

These conclusions are in agreement with the model proposed by Giorgetti et al. (2005) for residues from Phe375 to approximately Gln409 and with the model proposed by Hua and Gordon (2005) for residues from Gl417 to Val424. Conformational changes of these domains during channel gating have also a rotational component, as previously suggested (Johnson and Zagotta 2001; Nair et al. 2006).

Acknowledgments We are extremely thankful to Professor Vincent Torre for his generous support, advice, and constant encouragement. We thank Dr. Claudio Anselmi and Arin Marchesi for helpful discussions and Miss. M. Lough for reading the manuscript. This work was supported by a HFSP grant, a COFIN grant from the Italian Ministry, a grant from CIPE (GRAND FVG), and a FIRB grant from MIUR.

References

Akabas MH, Stauffer DA, Xu M, Karlin A (1992) Acetylcholine receptor channel structure probed in cysteine-substitution mutants. Science 258:307–310. doi:10.1126/science.1384130

Becchetti A, Roncaglia P (2000) Cyclic nucleotide-gated channels: intra- and extracellular accessibility to Cd^{2+} of substituted cysteine residues within the P-loop. Pflugers Arch 440:556–565

Becchetti A, Gamel K, Torre V (1999) Cyclic nucleotide-gated channels: pore topology studied through the accessibility of reporter cysteines. J Gen Physiol 114:377–392. doi:10.1085/jgp.114.3.377

Benitah JP, Tomaselli GF, Marban E (1996) Adjacent pore-lining residues within sodium channels identified by paired cysteine mutagenesis. Proc Natl Acad Sci USA 93:7392–7396. doi:10.1073/pnas.93.14.7392

Biel M, Zong X, Ludwig A, Sautter A, Hofmann F (1999) Structure and function of cyclic nucleotide-gated channels. Rev Physiol Biochem Pharmacol 135:151–171. doi:10.1007/BFb0033672

Bradley J, Frings S, Yau KW, Reed R (2001) Nomenclature for ion channel subunits. Science 294:2095–2096. doi:10.1126/science.294.5549.2095

Brown RL, Snow SD, Haley TL (1998) Movement of gating machinery during the activation of rod cyclic nucleotide-gated channels. Biophys J 75:825–833. doi:10.1016/S0006-3495(98)74064-0

Bucossi G, Eismann E, Sesti F, Nizzari M, Seri M, Kaupp UB, Torre V (1996) Time-dependent current decline in cyclic GMP-gated bovine channels caused by point mutations in the pore region expressed in Xenopus oocytes. J Physiol 493(Pt 2):409–418

Chen TY, Illing M, Molday LL, Hsu YT, Yau KW, Molday RS (1994) Subunit 2 (or beta) of retinal rod cGMP-gated cation channel is a component of the 240-kDa channel-associated protein and mediates Ca^{2+}-calmodulin modulation. Proc Natl Acad Sci USA 91:11757–11761. doi:10.1073/pnas.91.24.11757

Craven KB, Zagotta WN (2006) CNG and HCN channels: Two Peas, One Pod. Annu Rev Physiol 68:375–401. doi:10.1146/annurev.physiol.68.040104.134728

Craven KB, Olivier NB, Zagotta WN (2008) C-terminal movement during gating in cyclicc nucleotide-modulated channels. J Biol Chem 283(21):14728–14738. doi:10.1074/jbc.M710463200

Doyle DA, Morais CJ, Pfuetzner RA, Kuo A, Gulbis JM, Cohen SL, Chait BT, MacKinnon R (1998) The structure of the potassium channel: molecular basis of K^+ conduction and selectivity. Science 280:69–77. doi:10.1126/science.280.5360.69

Fesenko EE, Kolesnikov SS, Lyubarsky AL (1985) Induction by cyclic GMP of cationic conductance in plasma membrane of retinal rod outer segment. Nature 313:310–313. doi:10.1038/313310a0

Flynn GE, Zagotta WN (2001) Conformational changes in S6 coupled to the opening of cyclic nucleotide-gated channels. Neuron 30:689–698. doi:10.1016/S0896-6273(01)00324-5

Flynn GE, Zagotta WN (2003) A cysteine scan of the inner vestibule of cyclic nucleotide-gated channels reveals architecture and rearrangement of the pore. J Gen Physiol 121:563–582. doi:10.1085/jgp.200308819

Giorgetti A, Nair AV, Codega P, Torre V, Carloni P (2005) Structural basis of gating of CNG channels. FEBS Lett 579:1968–1972. doi:10.1016/j.febslet.2005.01.086

Hua L, Gordon SE (2005) Functional interactions between A' helices in the C-linker of open CNG channels. J Gen Physiol 125:335–344. doi:10.1085/jgp.200409187

Jiang Y, Lee A, Chen J, Cadene M, Chait BT, MacKinnon R (2002a) Crystal structure and mechanism of a calcium-gated potassium channel. Nature 417:515–522. doi:10.1038/417515a

Jiang Y, Lee A, Chen J, Cadene M, Chait BT, MacKinnon R (2002b) The open pore conformation of potassium channels. Nature 417:523–526. doi:10.1038/417523a

Johnson JP, Zagotta WN (2001) Rotational movement during cyclic nucleotide-gated channel opening. Nature 412:917–921. doi:10.1038/35091089

Karlin A, Akabas MH (1998) Substituted-cysteine accessibility method. Methods Enzymol 293:123–145. doi:10.1016/S0076-6879(98)93011-7

Kaupp UB, Seifert R (2002) Cyclic nucleotide-gated ion channels. Physiol Rev 82:769–824

Kaupp UB, Niidome T, Tanabe T, Terada S, Bonigk W, Stuhmer W, Cook NJ, Kangawa K, Matsuo H, Hirose T (1989) Primary structure and functional expression from complementary DNA of the rod photoreceptor cyclic GMP-gated channel. Nature 342:762–766. doi:10.1038/342762a0

Körschen HG, Illing M, Seifert R, Sesti F, Williams A, Gotzes S, Colville C, Müller F, Dose A, Godde M (1995) A 240 kDa protein represents the complete beta subunit of the cyclic nucleotide-gated channel from rod photoreceptor. Neuron 15:627–636. doi:10.1016/0896-6273(95)90151-5

Krovetz HS, VanDongen HM, VanDongen AM (1997) Atomic distance estimates from disulfides and high-affinity metal-binding sites in a K^+ channel pore. Biophys J 72:117–126. doi:10.1016/S0006-3495(97)78651-X

Kuo A, Gulbis JM, Antcliff JF, Rahman T, Lowe ED, Zimmer J, Cuthbertson J, Ashcroft FM, Ezaki T, Doyle DA (2003) Crystal structure of the potassium channel KirBac1.1 in the closed state. Science 300:1922–1926. doi:10.1126/science.1085028

Kurz LL, Zuhlke RD, Zhang HJ, Joho RH (1995) Side-chain accessibilities in the pore of a K^+ channel probed by sulfhydryl-specific reagents after cysteine-scanning mutagenesis. Biophys J 68:900–905. doi:10.1016/S0006-3495(95)80266-3

Long SB, Campbell EB, MacKinnon R (2005) Crystal structure of a mammalian voltage-dependent Shaker family K^+ channel. Science 309:897–903. doi:10.1126/science.1116269

Loo TW, Clarke DM (2001) Determining the dimensions of the drug-binding domain of human P-glycoprotein using thiol cross-linking compounds as molecular rulers. J Biol Chem 276:36877–36880. doi:10.1074/jbc.C100467200

Matulef K, Flynn GE, Zagotta WN (1999) Molecular rearrangements in the ligand-binding domain of cyclic nucleotide-gated channels. Neuron 24:443–452. doi:10.1016/S0896-6273(00)80857-0

Mazzolini M, Punta M, Torre V (2002) Movement of the C-helix during the gating of cyclic nucleotide-gated channels. Biophys J 83:3283–3295. doi:10.1016/S0006-3495(02)75329-0

Mazzolini M, Nair AV, Torre V (2008) A comparison of electrophysiological properties of the CNGA1, $CNGA1_{tandem}$ and $CNGA1_{cys\text{-}free}$ channels. Eur Biophys J 37(6):947–959. doi:10.1007/s00249-008-0312-1

Mazzolini M, Anselmi C, Torre V (2009) The analysis of desensitizing CNGA1 channels reveals molecular interactions essential for normal gating. J Gen Physiol 133(4):375–386. doi:10.1085/jgp.200810157

Nair AV, Mazzolini M, Codega P, Giorgetti A, Torre V (2006) Locking CNGA1 channels in the open and closed state. Biophys J 90:3599–3607. doi:10.1529/biophysj.105.073346

Nair AV, Anselmi C, Mazzolini M (2009) Movements of native C505 during channel gating in CNGA1 channels. Eur Biophys J 38(4):465–478. doi:10.1007/s00249-008-0396-7

Nakamura T, Gold GH (1987) A cyclic nucleotide-gated conductance in olfactory receptor cilia. Nature 325:442–444. doi:10.1038/325442a0

Roncaglia P, Becchetti A (2001) Cyclic-nucleotide-gated channels: pore topology in desensitizing E19A mutants. Pflugers Arch 441:772–780. doi:10.1007/s004240000480

Rosenbaum T, Gordon SE (2002) Dissecting intersubunit contacts in cyclic nucleotide-gated ion channels. Neuron 33:703–713. doi:10.1016/S0896-6273(02)00599-8

Rothberg BS, Shin KS, Phale PS, Yellen G (2002) Voltage-controlled gating at the intracellular entrance to a hyperpolarization-activated cation channel. J Gen Physiol 119:83–91. doi:10.1085/jgp.119.1.83

Rothberg BS, Shin KS, Yellen G (2003) Movements near the gate of a hyperpolarization-activated cation channel. J Gen Physiol 122:501–510. doi:10.1085/jgp.200308928

Shammat IM, Gordon SE (1999) Stoichiometry and arrangement of subunits in rod cyclic nucleotide-gated channels. Neuron 23:809–819. doi:10.1016/S0896-6273(01)80038-6

Zagotta WN, Siegelbaum SA (1996) Structure and function of cyclic nucleotide-gated channels. Annu Rev Neurosci 19:235–263. doi:10.1146/annurev.ne.19.030196.001315

Zheng J, Trudeau MC, Zagotta WN (2002) Rod cyclic nucleotide-gated channels have a stoichiometry of three CNGA1 subunits and one CNGB1 subunit. Neuron 36:891–896. doi:10.1016/S0896-6273(02)01099-1

Zhong H, Molday LL, Molday RS, Yau KW (2002) The heteromeric cyclic nucleotide-gated channel adopts a 3A:1B stoichiometry. Nature 420:193–198. doi:10.1038/nature01201

Zimmerman AL, Yamanaka G, Eckstein F, Baylor DA, Stryer L (1985) Interaction of hydrolysis-resistant analogs of cyclic GMP with the phosphodiesterase and light-sensitive channel of retinal rod outer segments. Proc Natl Acad Sci USA 82:8813–8817. doi:10.1073/pnas.82.24.8813